Asymmetrical Planetary Nebulae II: From Origins to Microstructures
ASP Conference Series, Vol. XXX, 2000
J.H. Kastner, N. Soker, & S. Rappaport, eds.

Molecular line observations of proto-planetary nebulae

J. Alcolea, V. Bujarrabal, A. Castro-Carrizo, C. Sánchez Contreras

Observatorio Astronómico Nacional (OAN), Apartado 1143, E–28800 Alcalá de Henares, Spain

R. Neri, J. Zweigle

Institute de Radio Astronomie Milimétrique, 300 Rue de la Piscine, F–38406 St. Martin d'Heres, France

Abstract.

We present our recent results on mm-wave CO observations of proto-planetary nebulae. These include high-resolution interferometric maps of various CO lines in three well known bipolar PPNe: M 1–92, M 2–56 and OH 231.8+4.2. The global properties of the high velocity molecular emission in post-AGB sources have been also studied, by means of high-sensitivity single dish observations of the J=1–0 and 2–1 lines of ^{12}CO and ^{13}CO. We discuss the implications of these results to constrain the origin of the post-AGB molecular high-velocity winds and the shaping of bipolar PPNe and PNe. In addition, we also present the results of an interferometric map of the molecular envelope around the luminous high-latitude star 89 Her, a low mass post-AGB source which is also a close binary system.

1. Introduction

After attending this conference, I think that everyone will agree that the subject of the origin of asymmetrical planetary nebulae, in particular the problem of the "shaping", is a matter of passionate debates, probably because our current observational knowledge of the problem still leads to too many possible solutions. From our point of view, this lack of knowledge is partially due to that planetary nebulae (PNe) themselves are not very good targets to study how this shaping process occurred. PNe are too old in two senses. On the one hand, regarding the problem of the shaping, we can consider PNe as mainly consisting in freely expanding gas: the interactions presently active do not bear information on the large-scale shaping process (the origin of the axis-symmetry, etc.). On the other hand, when observing gas in PNe, it is very difficult to detect more than just a little fraction of the total mass of the progenitor AGB envelope: we do not probe the whole dynamics.

One way to overcome these two difficulties is to study the objects in the phase between the AGB and PN stage, the proto-PNe (PPNe). Since they are younger, one expects them to show features of the more recent shaping processes, that could be even still active. They also have the advantage of being

rich in molecular content, because the central star is not hot enough to drive a strong photo-ionization in its envelope. Due to this, mm-wave observations of the emission from CO rotational lines can efficiently trace the bulk of the mass in the envelope. Traditionally, this type of observations was of limited use because PPNe are rare (the PPN phase is very brief, it lasts less than 2 000 yr), and therefore they are usually very far away and angularly small. Now, with instruments like the IRAM[1] Plateau de Bure (PdB) interferometer, we are able to image these sources with resolutions better than $1''$, providing simultaneously spectral resolutions better than 1 km s^{-1} and total mass sensitivities of the order of 0.01 $M_{\odot}$. Here we summarize our results from the CO mapping of several post-AGB envelopes using PdB: M 1–92, M 2–56, OH 231.8+4.2, and 89 Her (CO maps of CRL 2688 are also presented by Lucas et al. in this volume). For OH 231.8+4.2 we have also mapped lines other than CO; these chemical studies are outlined in the contribution by Sánchez Contreras et al. In addition, we also present the preliminary results of a survey of CO lines in post-AGB sources, carried out with the IRAM 30 m radiotelescope. We want to stress here the importance of this type of studies to understand PN shaping. Note that every PN was once a PPN, and that whatever the properties of these PPNe were, models trying to reproduce the final stage of a certain PN should predict PPN stages similar to those we do observe.

2. M 1–92: Minkowski's footprint

M 1–92 is a bipolar PPN with a 20 000 K central star, located 3 kpc away and with a luminosity of 10^4 $L_{\odot}$, that was known to show high velocity wings in molecular line emission. This is the object in which we started our mm-wave interferometric maps of PPNe, and therefore, the one we have studied in more detail. In addition to the high resolution maps of ^{12}CO and ^{13}CO we are discussing here, we have performed detailed imaging in the optical and NIR (using the WFPC2 and NICMOS2 on-board the HST), and continuum observations at 6 and 1.3 cm, and 2.6 and 1.3 mm (Alcolea et al. 1999).

The CO observations were conducted between 1993 and 1997, using the PdB interferometer, reaching a spatial resolution better than $1\farcs0$ in the ^{13}CO J=2–1 line (see Bujarrabal et al. 1994, 1997, 1998a). The quality of the data and the good spatial resolution in comparison with the total size of the nebula, $10''$, fully revealed the structure and kinematics of the molecular envelope, which consist of three main components (Fig. 1a). The densest parts of the nebula lie in an equatorial disk (or torus) dividing the two reflecting lobes; this equatorial structure is expanding radially, at a constant AGB-like velocity of 8 km s^{-1}. At both sides of this component, the reflecting lobes are surrounded by two molecular shells, elongated along the symmetry axis of the nebula, and showing a constant velocity gradient (7.5 km s^{-1} per $''$) in this direction. The walls of these shells are very thin ($0\farcs6$): the two shells are practically empty. The two lobes are ended by two high-velocity knots, moving at an expansion velocity of

[1]IRAM is an European institute for research in millimeter astronomy, funded by the CNRS (France), the MPG (Germany), and the IGN (Spain)

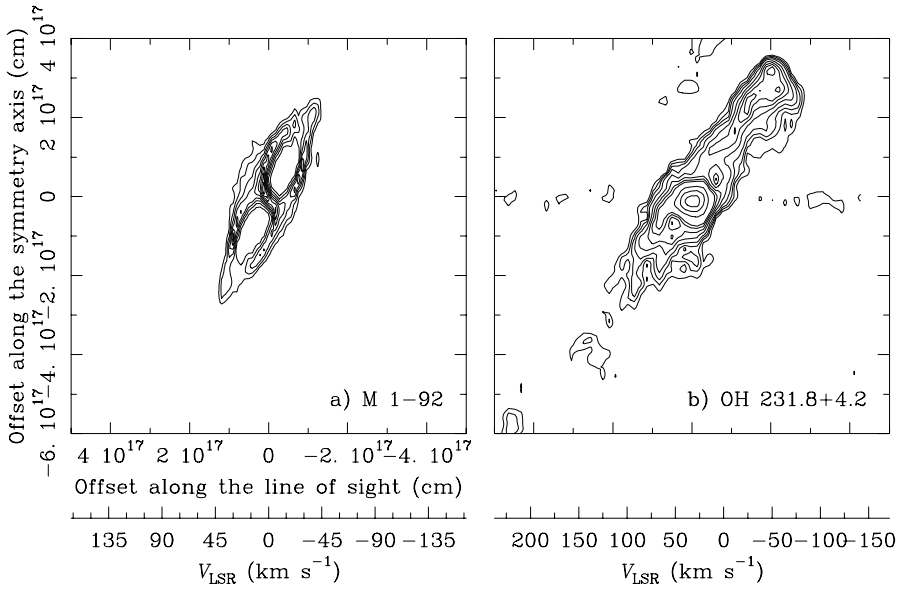

Figure 1. Velocity ($V_{\rm LRS}$) vs. position (projected distance) diagrams for cuts along the symmetry axis for M 1–92 (a) and OH 231.8+4.2 (b), showing their characteristic Hubble-like velocity law. Because of this law, distances along the line of sight can be recovered by simply assuming that the gas is radially expanding at a velocity directly proportional to the distance to the central source, i.e. $\vec{V} \propto \vec{R}$. To visualize the structure of the nebula under this assumption use the scale in cm in both axes

70 km s^{-1} along the axis. From the comparison of the different CO lines, we conclude that the kinetic temperature of the gas is very low, 10–30 K.

The total mass of the neutral nebula detected by the CO observations is 0.9 $M_\odot$, i.e., we are probably seeing the whole AGB envelope, strongly modified during the post-AGB evolution. We suggest that the present nebular configuration, which is only 900 yr old[2], is due to some post-AGB mass ejection, highly bipolar and very fast, which impinged on two opposite sites of the AGB shell, accelerating and stretching it along the newly formed axis of symmetry, via a momentum (quasi-isothermal) driven shock. Assuming that during the AGB the nebula was spherically symmetric, and expanded at the velocity now only present in the thick equatorial disk, the axial momentum won by the envelope during the post-AGB phase is $3\,10^{39}$ gr cm s^{-1}. This figure is nearly 10^2 times the amount of momentum available from photon pressure since the post-AGB interaction started. This result points out that not only the central star and the envelope change during the post-AGB evolution. The mass loss mechanism and its source of energy should also change, since photon pressure cannot account

[2]This is the kinematic age, Age$_{\rm kin}$, derived from the "constant" velocity gradient. This Hubble-like velocity field suggest that the interaction responsible for the present kinematics lasted much less than Age$_{\rm kin}$, i.e. $\lesssim$ 100–200 yr

for the observed momentum. We have detected in SII and OI lines the present bipolar post-AGB flow in M 1–92, as a chain of compact (0.″2) knots along the symmetry axis inside the CO empty shells (Bujarrabal et al. 1998b); the momentum carried by this wind is now very small, not affecting the kinematics of the envelope, but we cannot rule out that it were much larger in the past.

3. M 2–56

M 2–56 is also a PPN with a clear bipolar appearance in the optical, the axis of symmetry being oriented in the East-West direction. Located ~ 3 kpc away, the central star shows a B0 (30 000 K) spectral type and a luminosity of $10^4\ L_\odot$. In addition to PdB 4″ to 2″ resolution maps of the ^{12}CO J=1–0 and 2–1 emission, we have also performed spectro-imaging of optical lines tracing shocked excited gas. Our CO observations are still not finished (there are some additional data to be taken) and therefore their analysis is very preliminary. However, the main results outlined here should not change (Sánchez Contreras et al. in prep.).

From the CO maps, M 2–56 looks quite similar to M 1–92, except that in the former, only the central parts of the nebula and the high velocity knots at both ends of the axis of symmetry are clearly detected. The two empty shells, characteristic of M 1–92, appear weak and very fragmented in this case; they are mostly detected near the equatorial disk, which so resembles a sort of a flattened hourglass. Because of this lack of molecular emission between the equator and the poles of the nebula, and also because the symmetry axis lies almost in the plane of the sky, the constant velocity gradient is not so conspicuous here. However, when taking into account projection effects, we also obtain large values for the velocity gradient along the symmetry axis, 8.5 km s^{-1} per ″, the two high-velocity clumps escaping from the star at a velocity of 90 km s^{-1}. As for M 1–92, the equatorial disk shows radial expansion with an AGB-like velocity (8–15 km s^{-1}). We have measured a total envelope mass of 0.1 $M_\odot$, the corresponding axial momentum being $7\,10^{38}$ gr cm s^{-1}. From the velocity gradient, we estimate that M 2–56 is twice older than M 1–92: Age$_{\rm kin}$ $\sim$ 1 600–2 000 yr. This result agrees with other age indicators that also point out that M 2–56 should be more evolved than M 1–92; the bluer spectral type and the weaker CO emission. In fact, the most likely explanation for the nearly absence of molecular emission in the lobe walls, is that, because of this aging, photodissociation by UV radiation has partially destroyed the molecular envelope. We conclude that M 2–56 is an object very similar to M 1–92, and therefore originated in a similar way, but somewhat more evolved. In particular we suggest that the high-velocity knots detected in M 2–56, which are detached from the rest of nebula, could be progenitors of FLIERs.

4. OH 231.8+4.2

OH 231.8+4.2 is a very peculiar PPN. In the optical and NIR it shows a clear bipolar structure, but very asymmetric, the south lobe being more extended than the one in the north. The central star is also unique; located ~ 1.5 kpc away and with a luminosity of $10^4\ L_\odot$, it consists of a M9III Mira variable and

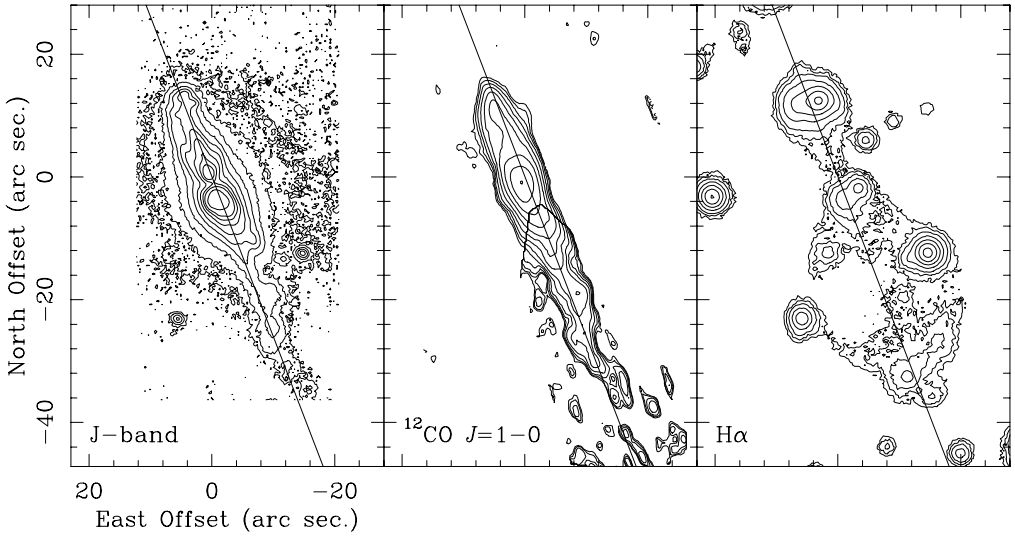

Figure 2. The circumstellar envelope of OH 231.8+4.2 as seen in the NIR (J-band, on the left) and in the total emission of the ^{12}CO J=1–0 line (center), in comparison with the optical appearance (Hα+continuum, on the right). Note the different extent of the two lobes at all wavelengths, the similitude between the NIR and CO images, and the different shape of the southern lobe in the optical

maybe a hotter companion (it could be a symbiotic system). Not surprisingly, this nebula is also very peculiar in molecular line emission, showing a very fast wind in CO and a particularly rich chemistry. In addition to PdB ^{12}CO high resolution maps, we have also performed interferometric observations of other molecular species (see the contribution by Sánchez Contreras et al.), and ground based optical long-slit observations and NIR imaging (Sanchez Contreras et al. 1999; some beautiful NIR images from the HST NICMOS2 camera have been presented by Bieging et al. in this conference). By the end of this year, we will also have HST WFPC2 images of the nebula in various atomic lines.

Our PdB interferometric maps of ^{12}CO J=1–0 and 2–1 are not so detailed as those of M 1–92 (partly because the low declination of the source), but are good enough as to show the structure of the nebula at a 2″ scale. The most outstanding feature of the molecular envelope is its shape; the CO nebula is extremely elongated, $1.6\,10^{18}$ cm long (along the symmetry axis) but only $1.5\,10^{17}$ cm across (taking into account an inclination of this axis with respect to the line of sight of 50–55°). This distribution of matter agrees very well with the ground based NIR images, but strongly contrasts with the optical picture, especially in the south lobe (Fig. 2). The kinematics of the molecular gas is dominated, once again, by the presence of a strong (8.9 km s^{-1} per ″, deprojected) and constant velocity gradient along the symmetry axis. We detect gas expanding up to 375 km s^{-1} in the south (210 km s^{-1} in the north): to our knowledge, this is the highest expansion velocity ever measured in molecular line emission from evolved stars. The total mass of the nebula is 0.5–1.0 $M_\odot$, and the axial momentum carried by the molecular flow, which is 750 yr old, is $3\,10^{39}$ gr cm s^{-1}.

Although the most remarkable feature in the maps is the presence of the very elongated fast emission in both lobes, the central core of the nebula is not less important. Because of the somewhat lower resolution attained for OH 231.8+4.2, the structure of the central parts of the nebula is not so clear. However, from the detailed inspection of the maps and its comparison with our first (also with $2''$ resolution) observations of M 1–92, we conclude that the two objects are very similar: there is a compact component at the very center of the nebula, and two hollow shells at both sides of it (Fig. 1b; see also the discussion of the HCO^+ observations in the contribution by Sánchez Contreras et al.). Therefore the main structural difference between the envelopes in M 1–92, M 2–56, and OH 231+8+4.2 is that, in the latter, the two high-velocity knots have been replaced by two asymmetrical jets expanding a high velocity. In any case, we suggest that the origin of the bipolarity of all three cases should be similar. The presence of the long high velocity CO jets in OH231.8+4.2 and not in the other two cases, could be due to differences in the details of the interaction responsible for the present shape (degree of collimation of the post-AGB jets, density contrast between the two colliding winds, etc.).

5. Global properties of the high-velocity CO emission in PPNe

The three objects just discussed provide many clues to investigate the origin of bipolar PPNe and PNe, suggesting a similar formation mechanism in all cases. However the sample is far from being statistically significant. Because of the relatively small number of dishes per instrument and total collecting area, one of today's problems in high-quality imaging in mm-interferometry is that it is highly time consuming. Typically, high quality imaging, like that performed in any of the four targets here presented, takes about 1.5–2.5 full days of observing time. Given the large observing pressure in this type of instruments, to map a large (statistically significant) sample of sources results prohibitive in these days. (This situation may change drastically if instruments like the planned ALMA become available.) To overcome these difficulties, we have carried out single dish observations, using the IRAM 30 m MRT, of a large number of PPNe, to study the global properties of the high-velocity molecular emission that characterizes this type of objects. The resolution of the telescope, $12''$, does not allow to map the sources in almost all cases, but under certain assumptions, one can determine the mass, momentum, and kinetic energy of the high velocity outflow. To better estimate the effects of line excitation and opacity, we have simultaneously observed the J=1–0 and 2–1 lines of ^{12}CO and ^{13}CO. "Very preliminary" results (Castro-Carrizo et al. in prep.) of these observations are summarized in Table 1.

In about 80% of the studied PPNe we have found high-velocity CO wings, with expansion velocities between 25 and 375 km s^{-1}. The derived total envelope mass can be as large as 0.5–1.0 $M_\odot$; in these cases it is clear that we have detected the whole circumstellar envelope. The measured axial momentum is always very large: the CO flows are "hyper-luminous" in the sense that the time required to obtain that momentum from photon pressure only ($\mathrm{Age}_{L_\star}$), 4 000–100 000 yr, is larger than the expected duration of the PPN phase. This problem becomes more severe if we consider the kinetic age ($\mathrm{Age}_{\mathrm{kin}}$) of the flows in those

objects in which it has been measured[3]. We note that the $\mathrm{Age}_{L_\star}$ – $P_{\mathrm{axial}}/(L_\star/c)$ – does not depend on the distance assumed for the source, which is the main source of uncertainty in all these computations.

Table 1. Summary of the results from the IRAM 30 m observations for sources showing high velocity molecular emission. Figures are corrected for distance, opacity, and axial inclination. V_{exp} is the maximum expansion velocity measured in CO; M_{CE} is the total mass of the molecular envelope; P_{axial} is the linear momentum along the axial directions; $\mathrm{Age}_{L_\star}$ is the time required for the photon pressure to account for the axial momentum, i.e. $P_{\mathrm{axial}}/(L_\star/c)$; $\mathrm{Age}_{\mathrm{kin}}$ is the kinetic age of the high velocity outflow when measured

Object name	V_{exp} ($\mathrm{km\,s^{-1}}$)	M_{CE} ($M_\odot$)	P_{axial} ($\mathrm{gr\,cm/s}$)	$L_\star$ ($L_\odot$)	$\mathrm{Age}_{L_\star}$ (yr)	$\mathrm{Age}_{\mathrm{kin}}$ (yr)
OH 231.8	375	1.0	$3\,10^{39}$	10^4	70 000	750
M 1–92	70	0.9	$3\,10^{39}$	10^4	70 000	950
M 2–56	90	.07	$7\,10^{38}$	10^4	30 000	1 800
Frosty Leo	235	.09	$9\,10^{38}$	$3\,10^3$	80 000	
He 3–1475	70	.07	$3\,10^{38}$	10^3	50 000	
IRC +10420	50	2.0	10^{40}	$7\,10^5$	5 000	
CRL 2688	190	0.7	$5\,10^{39}$	$4\,10^4$	30 000	
CRL 618	240	0.6	$2\,10^{39}$	$3\,10^4$	10 000	
IRAS 1743	28	0.6	$2\,10^{39}$	$6\,10^4$	6 000	
IRAS 1911	44	.04	$2\,10^{39}$	$3\,10^4$	20 000	
IRAS 1950	55	.03	$8\,10^{37}$	$2\,10^3$	10 000	
IRAS 2227	25	.07	10^{38}	$8\,10^3$	4 000	

These results, in addition to those obtained from the high resolution maps of PPNe (bipolarity, relative high degree of collimation, absence of large scale rotation in the envelopes), impose very strong constrains for the possible mechanisms capable of powering these molecular ejections, that we believe are also the responsible for the shaping of bipolar and point symmetric PNe. In fact, the large momentum and energy released in just a few hundred years rule out not only photon pressure, but probably all other mechanisms not powered by the accretion of material or by explosive nuclear reactions. On the other hand, the similitude between the post-AGB high-velocity molecular flows and those in young stellar objects, suggests that maybe also here the accretion of material is the right answer. So far, our observations do not tell us anything about the collimation mechanism except that it must be very efficient: in the southern jet of OH 231.8+4.2 the collimation factor is ~ 20; a similar number is found for the present post-AGB mass loss in M 1–92.

[3]Note that if our explanation for the Hubble-like velocity laws found in these objects is correct, i.e., the momentum transfer occurred in 100–200 yr or less, the problem is even worst

6. 89 Her

This object is the prototype of the so called luminous high-latitude stars (LHL), which are though to represent the post-AGB phase of low-mass stars, although maybe it cannot be considered as a low-mass PPN, since it is not clear whether this type of objects will evolve into PNe. 89 Her is a F2Ibe star (7 000 K) with a luminosity of 3 300 $L_{\odot}$ for an estimated distance of 600 pc (see Alcolea & Bujarrabal 1995 and references therein). The star is a regular pulsator with a period of 60 d and, based on an additional 288 d period of its radial velocity, it is believed to be a close binary system (Waters et al. 1993). The star was also known to present a strong IR excess due to a dusty circumstellar envelope, and a peculiar CO profile consisting of a very narrow component (FWHP ~ 3.5 km s^{-1}) plus weaker wings (FWZP ~ 20 km s^{-1}).

We observed this object with PdB in 1994–1995 using 4 antennas and in the 3 mm band only. We mapped the ^{12}CO J=1–0 line emission with a spatial resolution of $\sim 4''$ ($2''$ when using uniform weighting). The results of these observations are that the molecular envelope consists of two components: a compact core, only partially resolved by the observations, and a detached shell. Both components show, in first approximation, spherical symmetry, in spite of that 89 Her is a close binary system (see Alcolea & Bujarrabal 1995). This result does neither support nor rejects binarity as responsible for the bipolarity in PNe, but certainly supports the idea that maybe high-latitude (low-mass) objects are less likely to show strong deviations from spherical symmetry (Corradi & Schwarz 1995)

Acknowledgments. This work has been partially supported by the Spanish DGES project PB96-0104.

References

Alcolea J., & Bujarrabal V., 1995, A&A 303, L21

Alcolea J., & Bujarrabal V., 1999, in IAU Symp. 191, Asymptotic Giant Branch Stars, ed. T. le Bertre, A. Lèbre, & C Waelkens (San Francisco: ASP), 419

Bujarrabal V., Alcolea J., Neri R., & Grewing M., 1994, ApJ 436, L169

Bujarrabal V., Alcolea J., Neri R., & Grewing M., 1997, A&A 230, 540

Bujarrabal V., Alcolea J., & Neri R., 1998a, ApJ 504, 915

Bujarrabal V., Alcolea J., Sahai R., Zamorano J., & Zijltra A.A., 1998b, A&A 331, 361

Corradi R.L.M., & Schwarz H.E., 1995, A&A 293, 871

Sánchez Contreras C., Bujarrabal V., Alcolea J., Miranda F.L., & J. Zweigle, 1999, in IAU Symp. 191, Asymptotic Giant Branch Stars, ed. T. le Bertre, A. Lèbre, & C Waelkens (San Francisco: ASP), 347

Waters L.B.F.M., Waelkens C., Mayor M., & Trams N.R., 1993, A&A 269, 242